

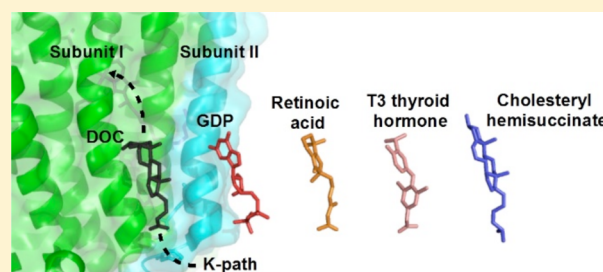
# Computational Prediction and *in Vitro* Analysis of Potential Physiological Ligands of the Bile Acid Binding Site in Cytochrome *c* Oxidase†

Leann Buhrow, Carrie Hiser, Jeffrey R. Van Voorst,<sup>¶</sup> Shelagh Ferguson-Miller,\* and Leslie A. Kuhn\*<sup>¶</sup>

Departments of Biochemistry and Molecular Biology and <sup>¶</sup>Computer Science & Engineering, Michigan State University, East Lansing, Michigan 48824, United States

## Supporting Information

**ABSTRACT:** A conserved bile acid site has been crystallographically defined in the membrane domain of mammalian and *Rhodobacter sphaeroides* cytochrome *c* oxidase (RsCcO). Diverse amphipathic ligands were shown previously to bind to this site and affect the electron transfer equilibrium between heme *a* and *a*<sub>3</sub> cofactors by blocking the K proton uptake path. Current studies identify physiologically relevant ligands for the bile acid site using a novel three-pronged computational approach: ROCS comparison of ligand shape and electrostatics, SimSite3D comparison of ligand binding site features, and SLIDE screening of potential ligands by docking. Identified candidate ligands include steroids, nicotinamides, flavins, nucleotides, retinoic acid, and thyroid hormones, which are predicted to make key protein contacts with the residues involved in bile acid binding. *In vitro* oxygen consumption and ligand competition assays on RscCo wildtype and its Glu101Ala mutant support regulatory activity and specificity of some of these ligands. An ATP analog and GDP inhibit RscCo under low substrate conditions, while fusidic acid, cholesteryl hemisuccinate, retinoic acid, and T3 thyroid hormone are more potent inhibitors under both high and low substrate conditions. The sigmoidal kinetics of RscCo inhibition in the presence of certain nucleotides is reminiscent of previously reported ATP inhibition of mammalian CcO, suggesting regulation involving the conserved core subunits of both mammalian and bacterial oxidases. Ligand binding to the bile acid site is noncompetitive with respect to cytochrome *c* and appears to arrest CcO in a semioxidized state with some resemblance to the “resting” state of the enzyme.



Cytochrome *c* oxidase (CcO) is the fourth complex of the electron transport chain responsible for reducing molecular oxygen to water and coupling this reaction to proton pumping.<sup>1,2</sup> CcO accepts electrons from cytochrome *c*, sequentially reduces its bimetallic copper A and heme *a* redox centers, and finally reduces the binuclear active site composed of heme *a*<sub>3</sub> and copper B (Figure 1). Two conserved proton paths, the D- and K-paths, have been identified in bacterial and mammalian oxidases. The K-path takes up one to two protons during active site reduction, while the D-path takes up all other protons consumed during oxygen reduction or pumped across the membrane.<sup>3–5</sup> A bifurcated oxygen channel leading from the membrane environment to the binuclear active site has been crystallographically defined.<sup>6,7</sup> A clear proton exit path has yet to be identified but may involve the heme propionate groups, propionate-associated water molecules, and/or a pair of arginines: Arg481 and Arg482 (*Rhodobacter sphaeroides* numbering is used unless otherwise noted).<sup>8–13</sup>

CcO is thought to be a key regulator of oxidative phosphorylation rate and efficiency.<sup>14–16</sup> In eukaryotic systems, CcO activity is modulated by the presence of alternative isoforms of nuclear-encoded accessory subunits,<sup>17–22</sup> phosphorylation at as many as 14 residues including three residues

on the conserved enzyme core,<sup>23,24</sup> and binding of small molecules.<sup>25–29</sup> A crystallographically defined small molecule site with a bound bile acid ligand (Figure 1) has been identified on both bacterial and mammalian CcO. This site is located in the membrane interface of subunits I and II, near the entrance to the K-path.<sup>30,31</sup> It has been hypothesized to natively bind nucleotides based on shape, chemistry, and binding preference similarities between ADP and bile acids;<sup>30</sup> however, no structural evidence of nucleotide binding has been obtained.

*R. sphaeroides* CcO (RsCcO) has been established as a useful model system to investigate the activity and regulation of mammalian CcO.<sup>32</sup> It is suitable for characterizing the bile acid site, as both bovine and *Rhodobacter* oxidases bind bile acids in the same region involving homologous amino acid residues.<sup>30,31,33</sup> RsCcO and its K-path mutant form, E101A, are activated or inhibited by a diverse group of ligands that appear to bind at the bile acid site, including detergents, fatty acids, steroids, and porphyrins.<sup>33,34</sup> RsCcO inhibition by these ligands and by mutations in the K-path has been attributed to an altered electron transfer equilibrium between heme *a* and *a*<sub>3</sub>

Received: May 29, 2013

Revised: August 23, 2013

Published: September 27, 2013



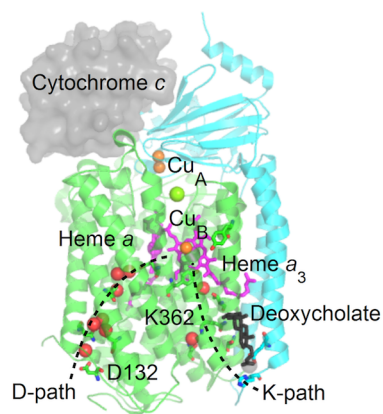


**Figure 1.** Structure of *R. sphaeroides* cytochrome *c* oxidase. The relative position of the cytochrome *c* substrate is represented by a gray surface, according to the docking analysis of Roberts and Pique, 1999.<sup>83</sup> *RsCcO* (PDB: 3DTU)<sup>31</sup> subunits I and II are depicted as green and cyan ribbons, respectively. Heme (magenta sticks) and copper (copper colored spheres) cofactors, crystallographic deoxycholate (gray sticks), and water molecules (red spheres) are also present. The conserved D- and K-paths for proton uptake are represented as dashed lines leading from the internal side of the membrane to the active site.

cofactors.<sup>33,35–37</sup> However, the native regulatory ligands for this conserved site remain elusive.

In order to understand the regulation of CcO at the bile acid site, a three-pronged computational approach was applied in this work to predict natural ligands with high complementarity to this conserved location. Initially, ligand comparisons were performed using the ROCS method<sup>38,39</sup> to identify candidate molecules that are structurally and chemically similar to the crystallographically bound bile acid. Second, protein comparisons and alignments were performed using the *SimSite3D* method<sup>40</sup> to search for binding sites that have similar shape and chemistry to the *RsCcO* bile acid site. The native ligands bound to these similar sites were then investigated for their interaction with the bile acid site. Finally, high ranking ligand candidates from both the ROCS and *SimSite3D* approaches were docked using *SLIDE*<sup>41,42</sup> to evaluate protein–ligand interactions. All commercially available, soluble, high scoring candidate ligands were tested for their ability to alter the rate of *RsCcO* oxygen consumption. Of these ligand candidates, a cholesterol mimic, a thyroid hormone, retinoic acid, and select nucleotides inhibit *RsCcO* activity. Ligand competition and mutational studies support the binding of these ligands to the bile acid site. Our studies suggest that this region may be polyspecific for a number of native regulatory ligands that arrest CcO activity by stabilizing an oxidized binuclear center. This semioxidized state has some resemblance to the “resting” state of the bovine enzyme and may have a lesser tendency for oxygen radical byproduct formation.

## MATERIALS AND METHODS

**Ligand Database Selection and Processing.** The Binding Mother of All Databases (Binding MOAD)<sup>43</sup> is a collection of thousands of crystallographic protein–ligand, protein–cofactor, and protein–ligand–cofactor complexes at or below 2.5 Å resolution. Binding MOAD includes physiologically relevant small molecules except for catalytic molecules (e.g., active site metals, hemes, porphyrins, etc.), covalently bound ligands, crystallographic additives (e.g.,

buffers, detergents, ions, etc.), and other macromolecules, defined as peptides longer than ten amino acids and DNA fragments larger than four nucleic acid residues. The redundant Binding MOAD database contains multiple copies of proteins with >90% sequence identity bound to different molecules and was used to maintain ligand diversity. Identical protein–ligand complexes were manually removed after analysis. This database was selected to assess molecules that complement the *RsCcO* bile acid site, as most of its molecules are natural compounds or analogs of natural compounds rather than synthetic molecules. However, this database is disadvantageous in that it does not contain porphyrin molecules, which have been shown to regulate *RsCcO* activity *in vitro*.<sup>33</sup>

**Geometric and Chemical Comparison of the *RsCcO* Bound Deoxycholate to Diverse Small Molecules.** Rapid Overlay of Chemical Structures (ROCS version 2.4.2; OpenEye Scientific Software, Santa Fe, NM) aligns a database of molecules or molecular conformations to a reference ligand structure based on maximizing shape and chemical similarity.<sup>38,39</sup> Ligands are represented by a Gaussian atomic density function about each atom center<sup>38</sup> and aligned such that they have maximal overlap, calculated as in Grant et al., 1996.<sup>39</sup> This overlap is assessed by a Tanimoto or Tversky scoring metric, based on whether overall or substructure matching is desirable. Tanimoto scores, a variation of the Jaccard index, describe the correlation between vectors with continuous or binary attributes representing molecular shape and chemistry. The geometric (ShapeTanimoto) and chemical (ColorTanimoto) similarities are independently scored and scaled between zero and one,<sup>38</sup> resulting in a maximum combined score (TanimotoCombo) of two for exact ligand matches.

ROCS was applied to identify physiological ligands similar in shape or electrostatics to deoxycholate (DOC). The *RsCcO*'s bound DOC (Protein Data Bank (PDB): 3DTU<sup>31</sup>) was compared to the crystallographic ligands in Binding MOAD and all low energy conformers of these ligands, as determined by *Omega* v 2.4.2 (OpenEye Scientific Software, Santa Fe, NM).<sup>44</sup> TanimotoCombo score was used to rank the resultant ligand conformations, equally weighing shape and chemical complementarity. All ligands scoring three standard deviations or greater than the average ROCS TanimotoCombo score across the entire Binding MOAD database were grouped into dominant chemical classes (e.g., bile acids, steroids, etc.) with redundant ligands removed. Ligands were selected for testing based on TanimotoCombo score ranking, commercial availability, and ability to be solubilized at a concentration sufficient for assaying ( $\geq 100 \mu\text{M}$ ).

**Chemical and Shape Comparisons of the *RsCcO* Bile Acid Site and Diverse Crystallographic Sites.** The second method used to assess candidate ligands, *SimSite3D*, is a protein binding site alignment and comparison tool that identifies a ranked list of sites most similar to the site of interest. Each site is represented using a set of pharmacophore points with associated bonding geometry and an accompanying solvent accessible molecular surface representing the detailed shape of the site.<sup>40</sup> The pharmacophore points denote positions where non-hydrogen atoms, of the appropriate chemistry, may be placed to form favorable polar or hydrophobic interactions with atoms in the protein. Polar pharmacophore points have an associated optimal hydrogen-bond direction, used to scale the energy estimate of the hydrogen bond according to its degree of linearity, while the molecular surface matching term ensures

that highly ranked sites will have a shape very similar to that of the site of interest.<sup>40</sup>

The RsCcO bile acid site was defined about the DOC crystallographic ligand (PDB: 3DTU).<sup>31</sup> The *SimSite3D* default protocol for template generation was used and included all pharmacophore points within 3.0 Å of at least one non-hydrogen atom of DOC. The molecular surface of the site, within 4.0 Å of DOC, was computed using the MSMS method.<sup>45</sup> Binding MOAD sites' pharmacophore points were optimally aligned to the pharmacophore points of the RsCcO bile acid site by *SimSite3D* into the RsCcO frame of reference. All ligand sites found in Binding MOAD were ranked based on *SimSite3D* score, calculated as

$$\text{SimSite score} = -2.62899 - 0.0122689\alpha - 0.00619202\beta + 2.11849\gamma$$

where  $\alpha$  is the sum of the number of matched hydrogen bond donor and hydrogen bond acceptor groups,  $\beta$  is the sum of matched chemical groups that may serve as either hydrogen bond donor or acceptor groups, and  $\gamma$  is the root mean squared error between aligned surfaces which also reflects hydrophobic surface matching.<sup>40</sup> Of the thousands of protein sites from Binding MOAD analyzed by *SimSite3D*, those sites scoring two standard deviations greater than the average *SimSite3D* score across Binding MOAD were analyzed as the best candidates for being physiologically relevant. These sites were grouped into dominant chemical classes (e.g., steroid, nucleotide, or lipid binding proteins), with redundant protein–ligand crystallographic complexes removed.

**Small Molecule Docking of Predicted Ligands into the RsCcO Bile Acid Site.** In the third approach to identify physiological ligand candidates, the RsCcO bile acid site with bound DOC removed (PDB: 3DTU)<sup>31</sup> was used as the target for *SLIDE* (Screening Ligands by Induced-fit Docking, Efficiently)<sup>41,42</sup> prediction of the binding modes of ROCS and *SimSite3D* candidate ligands. Similar to the *SimSite3D* representation, *SLIDE* characterizes favorable positions for protein–ligand hydrophobic interactions or hydrogen bonds in a binding pocket by generating a template of chemistry-labeled points. To fully sample candidate ligand flexibility, *Omega* v 2.4.2 was used to generate all low-energy conformations of the ligands prior to docking. *SLIDE* predicts the ligand binding orientation for each molecule by first sampling all matches between triplets of ligand atoms with complementary chemical type and interatomic distance to triplets of protein template points, resulting in alternative dockings that exhibit shape and chemical complementarity between the protein and ligand. The best orientation is then chosen according to the most favorable  $\Delta G_{\text{binding}}$  value according to *SLIDE*'s OrientScore [Tonero, Zavodszky, Van Voorst, He, Arora, Namilikonda, and Kuhn, *in preparation*]. *SLIDE*'s AffiScore then ranks the ligand candidates by a more detailed weighted sum of favorable hydrophobic and hydrogen-bonding interaction terms and unfavorable (unsatisfied/repulsive) interaction terms between the protein and docked ligand to assess their relative  $\Delta G_{\text{binding}}$ . Additionally, the dominant interactions between the diverse docked ligands and the RsCcO bile acid site were tabulated according to frequently contacted protein residues.

**RsCcO Purification and Oxygen Consumption Activity Assays.** *R. sphaeroides* strains overexpressing the 37–2 wild-type (WT) CcO<sup>46</sup> and E101A mutant<sup>47</sup> were grown as previously described. Cell membranes were prepared and

RsCcO was isolated by metal affinity chromatography as described for crystallographic studies.<sup>47</sup> Oxygen uptake rates were measured with a Clark-type electrode, and turnover rates (TN in electrons per second per CcO molecule) were calculated as described in Hosler et al., 1992.<sup>32</sup> Assay mixtures contained 100 mM HEPES pH 7.4, 24 mM KCl, 2.8 mM ascorbate, 1 mM *N,N,N',N'*-tetramethyl-*p*-phenylenediamine (TMPD), 5.6  $\mu$ M EDTA, 0.01% lauryl maltoside (LM), with 0–30  $\mu$ M purified bovine heart cytochrome *c* as the substrate and other additives as noted. Farnesyl diphosphate was purchased from Echelon Biosciences Incorporated (Logan, UT). All other additives were from Sigma-Aldrich (St. Louis, MO). Cholesteryl hemisuccinate and mammalian steroid hormones were dissolved in ethanol, retinoic acid was dissolved in DMSO, T3 thyroid hormone was dissolved in 0.1 N NaOH, and all other ligands were dissolved in water. Ligand effects were determined by the change in activity compared to an equal volume of the solvent alone. *Prism* v 6 (Graphpad Software, La Jolla, CA) was used to calculate kinetic values. Ligand titrations were fit with allosteric sigmoidal least-squares regression, and IC<sub>50</sub> values were reported. Cytochrome *c* titrations were fit with the mixed inhibition model, a general form of noncompetitive inhibition, with least-squares regression and reported K<sub>i</sub> values.

## RESULTS

**Chemical and Geometric Comparisons Between the CcO Crystallographic Deoxycholate and Diverse Ligands.** Mammalian and bacterial CcO proteins have been crystallized in the presence of bile acids, cholate in the case of bovine CcO (bovCcO),<sup>30</sup> and DOC in the case of RsCcO.<sup>31</sup> The ability of bile acids to bind to a conserved site and inhibit activity invokes the hypothesis that they mimic structurally similar, native regulatory molecules. In order to understand which potential physiological ligands are significantly similar to the bound DOC, the ROCS method was used to evaluate chemical and geometric similarities between DOC and ligands in the Binding MOAD database. Six chemical classes of ligands were identified, including bile acids, steroids, retinoic acid analogs, amino acid analogs, nucleotide and flavin analogs, and thyroid hormone analogs (Table 1 and SI Table 1). ROCS alignments of these predicted ligands to the crystallographic DOC resulted in an overlay of polycyclic ligand groups with the DOC steroid ring system and aliphatic, carboxylate, or phosphorylated ligand tails with the DOC carboxylate tail (Figure 2 and SI Figure 1). It had been suggested previously that the bile acid site is in fact an allosteric regulatory site that binds ADP under physiological conditions.<sup>30</sup> The similarity between DOC and abundant adenine-containing ligands and nucleotides was also evaluated by ROCS with thirteen nucleotides, FAD, and an NAD<sup>+</sup> analog scoring highly structurally and chemically similar to DOC (SI Table 2).

**Chemical and Geometric Comparisons Between the CcO Bile Acid Site and Diverse Protein Sites.** In order to predict varied candidate ligands that complement RsCcO, rather than just those similar to DOC, the CcO bile acid binding site was compared to diverse ligand sites in Binding MOAD using the *SimSite3D* method. *SimSite3D* compares crystallographic protein sites based on surface chemistry and geometry, using no knowledge of the existing bound ligand or the underlying amino acid sequence.<sup>40</sup> This approach identified five classes of protein sites, characterized by their bound flavin, lipid, nicotinamide, nucleotide, and steroid ligands (Table 1 and



**Table 1. Chemical Classes of Top Predicted Ligand Candidates<sup>a</sup>**

method	ligand class	number of ligands in top scoring results	average Tanimoto combo score
ROCS	Bile acids	10	1.17
	Steroids	31	0.96
	Retinoic acid analogs	5	0.94
	Amino acid analogs	8	0.91
	Nucleotide and flavin analogs	6	0.9
	Thyroid hormone analogs	2	0.87
			average SimSite3D score
SimSite3D	Nicotinamides	55	−2.43
	Flavins	24	−2.31
	Lipids	21	−2.27
	Nucleotides	44	−2.24
	Steroids	5	−2.07

<sup>a</sup>The first panel lists ROCS-analyzed ligands scoring at least three standard deviations above the average TanimotoCombo score across Binding MOAD ( $\geq 0.85$ ; where more positive scores indicate greater ligand similarity). The second panel lists SimSite3D protein binding site matches scoring at least two standard deviations below the average SimSite3D score across Binding MOAD ( $\leq -2.00$ ; where more negative scores indicate greater site similarity).

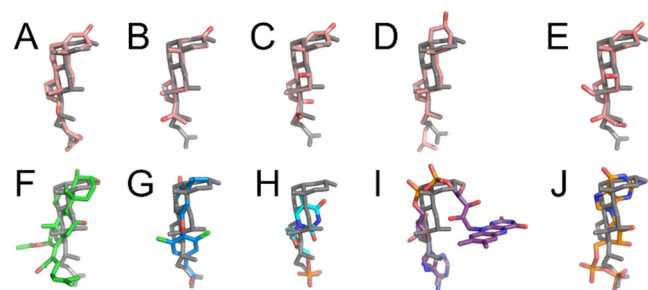


**Figure 2.** Biological ligands highly similar in shape and chemistry to the CcO crystallographic deoxycholate. The RsCcO bound DOC and Binding MOAD steroids, retinoic acid, thyroid hormone, nucleotides, and flavins were found to be significantly similar in shape and chemistry as determined by ROCS. The top ranked ligands: (A) testosterone hemisuccinate, (B) progesterone, (C) hydrocortisone, (D) cholesterol, (E) aldosterone, (F) fusidic acid, (G) thyroid hormone, (H) retinoic acid, (I) FAD, and (J) GDP are shown as aligned by ROCS to the crystallographic DOC (gray sticks).

SI Table 3). Interestingly, no bile acid binding proteins were identified as high scoring by SimSite3D. Striking overlap between the ROCS and SimSite3D ligand candidates is observed as both methods identified hydrocortisone, cholesterol, aldosterone, FAD, NAD<sup>+</sup>, GDP, ATP, and ADP, despite ROCS only using DOC ligand information and SimSite3D only using knowledge of the RsCcO bile acid site with DOC removed.

**Prediction of Critical Amino Acid Residues and Candidate Ligand Binding Orientations in the CcO Bile Acid Site.** The ROCS method of ligand comparison and SimSite3D method of protein site comparison identified candidate ligands with the potential to affect CcO by specifically interacting at the bile acid site. However, neither of these

results provided information about the interactions between the candidate ligands and the amino acid side chains of the CcO bile acid site. To understand the binding orientation and relative energetic favorability of candidate molecules, these ligands were docked into the RsCcO bile acid site with SLIDE. The docked ligands interacted with eight residues: P315 and Y318 in subunit I and H96, S98, E101, I102, W104, and T105 in subunit II (Table 2). Additionally, the diverse protein sites aligned to RsCcO by SimSite3D indicate that five residues, based on aligned chemical groups, are responsible for the dominant chemical interactions in the bile acid site. These residues are P315 in subunit I and H96, S98, E101, and T105 in subunit II (Figure 3). The consensus between SLIDE docking and SimSite3D alignment of five amino acids supports the role of these residues in ligand binding and will guide mutagenesis efforts in subsequent work.

In addition to the identification of five consensus residues in the bile acid site, SimSite3D alignment suggests variation in hydrophobic and hydrophilic ligand binding. The SimSite3D protein site classes that bound flavin, nicotinamide, or nucleotide ligands contained chemical groups analogous to the five dominant residues in the bile acid site (Table 3). Lipidic or steroidal ligand binding sites, from the mostly soluble proteins in Binding MOAD, were less similar to the bile acid site, as these sites matched fewer CcO residues. These results suggest that either this site may be more complementary to hydrophilic ligands despite its location in the membrane domain or the Binding MOAD database entries from the PDB, containing mostly soluble proteins, have insufficient examples of hydrophobic ligand binding sites for a comprehensive comparison. Nevertheless, hydrophobic and amphipathic ligands have the strongest effect on RsCcO activity under the *in vitro* assay conditions used (in this work and Hiser et al., 2013<sup>33</sup>). The results raise the possibility that the CcO bile acid site may interact with hydrophobic ligands such as lipids or steroids more strongly when in contact with the membrane/detergent environment, but may change in affinity and specificity toward hydrophilic ligands when the membrane environment is interrupted by protein/protein interactions upon formation of dimers and higher molecular weight complexes.<sup>30,48</sup>

Interestingly, both the SimSite3D protein site comparison and SLIDE docking methods identified similar binding orientations among the analyzed riboside ligands (Figure 4). By optimally aligning protein sites with SimSite3D and including the crystallographic bound ligands in the same reference frame, the approximate ligand binding orientations can be inferred and compared to ligand dockings. Riboside ligands interacted with the RsCcO bile acid site via (1) the ligand phosphate groups with H96 and E101, (2) the ligand ribose with T105, and (3) the ligand nitrogenous base or other cyclic group with the P315 hydrophobic pocket. The identification of similar binding orientations using two independent methods and between structurally similar ligands suggests there are conserved features of ADP, ATP, GDP, FAD, and NAD<sup>+</sup> binding in the CcO steroid binding site.

**In Vitro Assay of CcO Regulation by the Candidate Ligands.** ROCS ligand comparisons and SimSite3D protein site comparisons identified an overlapping but diverse set of candidate ligands (Table 1). To assess the ability of high scoring, commercially available ligands to act as regulators, the oxygen consumption activity of RsCcO was monitored at saturating cytochrome *c* concentrations in the presence and

Table 2. *SLIDE* Docked Ligands and Their Protein Interactions<sup>a</sup>

ligand	interacting fragment	OrientScore	AffiScore	percentage of docked ligand interactions							
				subunit I		subunit II					
				P315	Y318	H96	S98	E101	I102	W104	T105
ADP	Adenine	−8.0	−7.0	100	33	100	100	100	100	33	10
ATP	Adenine	−8.7	−7.9	88	77	100	88	100	85	62	77
GDP	Guanine	−8.1	−7.1	90	90	90	40	80	50	80	60
GDP	None	−8.1	−7.5	100	14	100	71	79	0	0	7
FAD	Adenine	−9.7	−10	83	50	83	83	100	67	0	67
FAD	Flavin	−9.2	−9.9	100	82	91	64	100	64	41	55
NAD <sup>+</sup>	Adenine	−9.3	−8.6	100	54	100	87	97	79	36	90

<sup>a</sup>*SLIDE* was used to dock riboside candidate ligands into the RsCcO steroid binding site. The top scoring binding orientations were characterized as scoring two standard deviations or better than the average *SLIDE* OrientScore for an individual molecule. AffiScore is the predicted  $\Delta_{\text{binding}}$  from *SLIDE*. These top scoring dockings were divided based on whether the bound ligand fragment was a nucleic acid base, flavin moiety, or neither. The percentage of ligands interacting with the eight most frequently contacted RsCcO residues is listed.

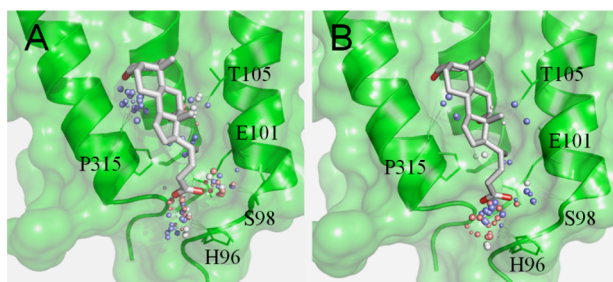


**Figure 3.** *SimSite3D* points of similar chemistry between the RsCcO bile acid binding site and top-scoring ligand site matches from Binding MOAD. (A) Points of chemical interaction in RsCcO surrounding subunit I residue P315 and subunit II residues H96, S98, E101, and T105 were frequently matched by nicotinamide, nucleotide, and flavin binding sites. (B) Steroid and lipid binding sites frequently matched the chemistry near RsCcO bile acid binding site residue P315 in subunit I and H96 and S98 in subunit II. Small blue and red spheres indicate matched positions for hydrogen-bond donors and acceptors in the top-scoring sites, respectively. White spheres indicate matched hydrogen bond donor and/or acceptor (e.g., hydroxyl group) sites. The crystallographically defined DOC is shown in light gray sticks.

Table 3. Percentage of Protein Binding Sites Matches Between the CcO Bile Acid Site and Diverse Binding MOAD Sites.<sup>a</sup>

CcO residue	nucleotide sites	nicotinamide sites	flavin sites	steroid sites	lipidic sites
P315	52	63	87	60	36
H96	70	91	100	60	100
S98	54	67	65	60	29
E101	66	100	50	0	29
T105	96	100	65	20	19

<sup>a</sup>*SimSite3D* aligns ligand binding sites based on the site's chemically labeled template points and the solvent-accessible molecular surface. The aligned points between the CcO bile acid site and diverse proteins in Binding MOAD may then be mapped back to individual residues. Five CcO residues were identified as being shared by high-scoring, diverse sites. The percentage of sites sharing a given residue interaction is tabulated.

absence of individual candidate ligands (Figure 5). An ATP analog [adenosine 5'-( $\beta,\gamma$ -imido) triphosphate] and GDP were assayed at physiological millimolar concentrations,<sup>49</sup> similar to those previously observed to regulate mammalian CcO *in vitro*.<sup>25–27,50,51</sup> Both ligands inhibited activity of RsCcO under

saturation cytochrome *c* concentrations to a similar limited extent (Figure 5A) with similar affinities (Figure 5B), as assessed by the half maximal inhibitory concentration for the ATP analog ( $IC_{50} = 4.4$  mM) and GDP ( $IC_{50} = 4.6$  mM). Fusidic acid ( $IC_{50} = 3.4$  mM), cholesteryl hemisuccinate (CHS;  $IC_{50} = 240$   $\mu$ M), retinoic acid ( $IC_{50} = 1.7$  mM), and T3 thyroid hormone ( $IC_{50} = 210$   $\mu$ M) are more potent inhibitors, some in the micromolar range. Other predicted ligands including ADP, FAD, farnesyl diphosphate, NAD<sup>+</sup> (Figure 5A), and the hydrophobic steroids testosterone, estradiol, hydrocortisone, and aldosterone (SI Figure 2) had no significant effect.

Retinoic acid, fusidic acid, and the ATP analog elicited a biphasic response: activation at low ligand concentration followed by inhibition at higher concentration (Figure 5B). This behavior has been observed previously upon addition of amphipathic ligands to the RsCcO mutant, E101A, under standard assay conditions (0.06% LM) and to WT in 0.01% detergent (Figure 6). This initial activation effect in E101A has been attributed to chemical rescue by carboxyl group replacement and the displacement of inhibitory detergent, while the subsequent inhibition is hypothesized to result from a ligand-specific effect.<sup>33</sup> Detergent sensitivity of the larger, more hydrophobic bile acid site in the E101A mutant, but not in the WT, has been demonstrated.<sup>33</sup> Additionally, detergent sensitivity to biphasic ligand-induced effects is only observed in the E101A mutant and not in the WT enzyme.<sup>52</sup> These results suggest that biphasic effects of ligands binding to the WT enzyme are due to more than one interaction mode, activating at low concentrations and inhibiting at high concentrations, independently of detergent. Yet these biphasic effects are associated with the bile acid region since both are altered by the E101A mutation (Figure 6 and see below). Clearer understanding of this complex activation/inhibition behavior awaits further structural and mutagenic studies.

**Mutation and Ligand Competition Analyses Support Binding to the Bile Acid Site.** The three-pronged computational approach was applied to identify biological ligands that may regulate CcO at the bile acid site. To test the binding location of the CcO inhibitors predicted in this work, a form of the RsCcO with a mutation in one of the five consensus bile acid residues (Table 2 and Figure 3), E101A, was monitored for ligand-induced activity changes. In addition to E101 being identified as a key residue by both *SimSite3D* and *SLIDE*, its mutant form has been shown to be a sensitive system for investigating ligand binding to the bile acid site.<sup>33</sup> When assayed with the E101A mutant, the ATP analog and GDP



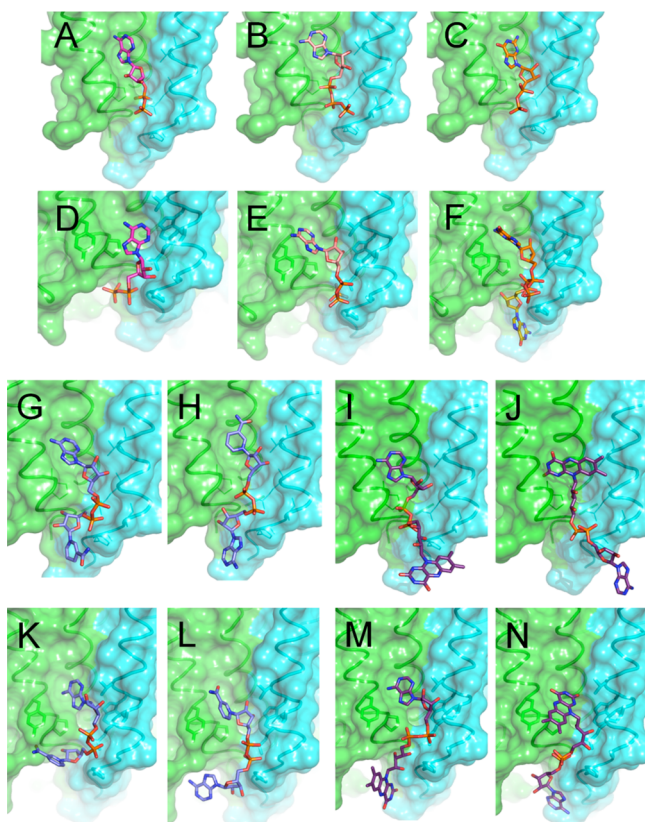


**Figure 4.** Binding modes predicted by *SimSite3D* site alignment and *SLIDE* docking. For each of the nucleotides,  $\text{NAD}^+$ , and FAD, *SimSite3D* and *SLIDE* predicted similar binding modes. In all cases, the di- or triphosphate groups are bound near the entrance of the K-path, specifically near H96 and E101. The ribose group was bound in the center of the steroid binding site and interacted with T105. Finally, the nucleic acid base, nicotinamide, or flavin moiety was located farthest into the membrane domain, often interacting near P315. The subunit I (green ribbon)/subunit II (cyan ribbon) interface is depicted with interacting amino acid residues in stick diagram. Binding modes determined by *SimSite3D*: (A) ADP (magenta sticks), (B) ATP (salmon sticks), (C) GDP (orange sticks), (G, H)  $\text{NAD}^+$  (blue sticks), and (I, J) FAD (purple sticks). Binding modes determined by *SLIDE* are shown immediately below the *SimSite3D* orientation for the same ligand: (D) ADP (magenta sticks), (E) ATP (salmon sticks), (F) GDP (orange sticks), (K, L)  $\text{NAD}^+$  (blue sticks), and (M, N) FAD (purple sticks). Note that (F) the *SLIDE* docking of GDP also predicted a binding orientation with the nitrogenous base extended into the aqueous surroundings (yellow sticks).

showed very low stimulation and no inhibition of activity.<sup>52</sup> The cholesterol mimic CHS ( $\text{IC}_{50} = 530 \mu\text{M}$ ) still inhibited the mutant but with reduced affinity (Figure 6). These lower binding affinities are consistent with the predicted dominant role of E101 in hydrophilic ligand binding to the bile acid site (Tables 2 and 3). In contrast, both retinoic acid ( $\text{IC}_{50} = 190 \mu\text{M}$ ) and T3 thyroid hormone ( $\text{IC}_{50} = 66 \mu\text{M}$ ) appeared to bind more tightly to the mutant, as might be expected based on the predicted lesser dependence of lipidic ligands on E101 (Table 3) and the increased overall hydrophobicity of the site. In all cases, the mutation had a significant influence on the ligand behavior, consistent with the predicted characteristics of the bile acid site.

To further test the localization of nucleotide binding to the bile acid site, the ability of the crystallographically observed DOC ligand to inhibit *RsCcO* activity was monitored in the

presence and absence of the ATP analog. DOC is a stronger inhibitor ( $\text{IC}_{50} = 1.4 \text{ mM}$ ) than the ATP analog ( $\text{IC}_{50} = 4.4 \text{ mM}$ ) and can lower *RsCcO* activity by more than 90% (Figure 7). At 5 mM concentration, the ATP analog alone elicits no effect as this is the midpoint of the ligand's biphasic affect (Figure 5B). However, at this concentration, the ATP analog prevented DOC in the 0–2 mM range from inhibiting *RsCcO* activity, showing its ability to compete with the bile acid (Figure 7). Together, the DOC competition and the effects of the E101A mutation support the prediction that nucleotides bind at the bile acid site and that both their initial activation and subsequent inhibition of *CcO* is mediated by this region.

#### Nonsaturating Cytochrome *c* Concentrations Reveal Sigmoidal and Noncompetitive Patterns of Inhibition.

The regulation of mammalian *CcO* by nucleotides and thyroid hormone has been observed previously by investigating ligand effects at a range of nonsaturating to saturating levels of cytochrome *c*.<sup>25–27,50,51</sup> As the present work has discovered nucleotide effects on bacterial *CcO*, all candidate ligands were further tested for their ability to influence *RsCcO* activity at nonsaturating cytochrome *c* concentrations. Fusidic acid ( $K_i = 2.5 \text{ mM}$ ), CHS ( $K_i = 290 \mu\text{M}$ ), retinoic acid ( $K_i = 140 \mu\text{M}$ ), and T3 thyroid hormone ( $K_i = 30 \mu\text{M}$ ) were observed to be strong inhibitors at all substrate concentrations (Figure 8A; SI Table 4), while  $\text{NAD}^+$  (Figure 8A) and the hydrophobic steroids testosterone, estradiol, hydrocortisone, and aldosterone (data not shown) failed to affect *RsCcO* under low or high concentrations of cytochrome *c*. In contrast, physiological concentrations of ADP ( $K_i = 3.1 \text{ mM}$ ), the ATP analog ( $K_i = 1.5 \text{ mM}$ ), and GDP ( $K_i = 1.7 \text{ mM}$ ) inhibited *RsCcO* most strongly at cytochrome *c* concentrations below  $15 \mu\text{M}$  (Figure 8B; SI Table 4). The effects of these ligands were fit with noncompetitive inhibition, selected as its regression better described the activity with nonsaturating cytochrome *c* levels, compared to competitive inhibition models.

Under these assay conditions, *RsCcO* inhibition by nucleotides gives rise to a sigmoidal curve (Figure 8B), similar to the behavior observed in mammalian *CcO* in the presence of ATP.<sup>25–27,50,51</sup> Originally, this sigmoidal inhibition of *bovCcO* was argued to represent negative cooperativity between cytochrome *c* substrate binding sites on the mammalian dimer elicited by ATP binding on the matrix domains of nuclear-encoded subunits IV or VI.<sup>26,27</sup> Allosteric regulation of bacterial *CcO* by nucleotides had not been observed prior to this study. This lack of inhibition was suggested to be due to the absence of nuclear-encoded subunits containing the ATP regulatory sites.<sup>53</sup> However, the sigmoidal curves observed in nonsaturating cytochrome *c* assays of *RsCcO* in the presence of nucleotides suggests that this inhibitory effect must be due to ligand binding on the core subunits of the *CcO*, potentially at the bile acid site.

DOC inhibition of the *RsCcO* WT and the E101A mutant (Figure 9) is also consistent with noncompetitive inhibition with respect to cytochrome *c*, characterized by an altered  $V_{\text{max}}$  but no change in apparent  $K_m$  for cytochrome *c*. Additionally, the T3 thyroid hormone noncompetitively inhibits the *RsCcO* WT (data not shown). These results suggest that *CcO* inhibition by ligand binding to the bile acid site, including the sigmoidal inhibition by nucleotides, is unlikely to be explained by allosterically altered cytochrome *c* affinity. An alternative model consistent with the kinetic, crystallographic,<sup>33</sup> and spectral studies<sup>33,35–37</sup> is preferential ligand binding to the

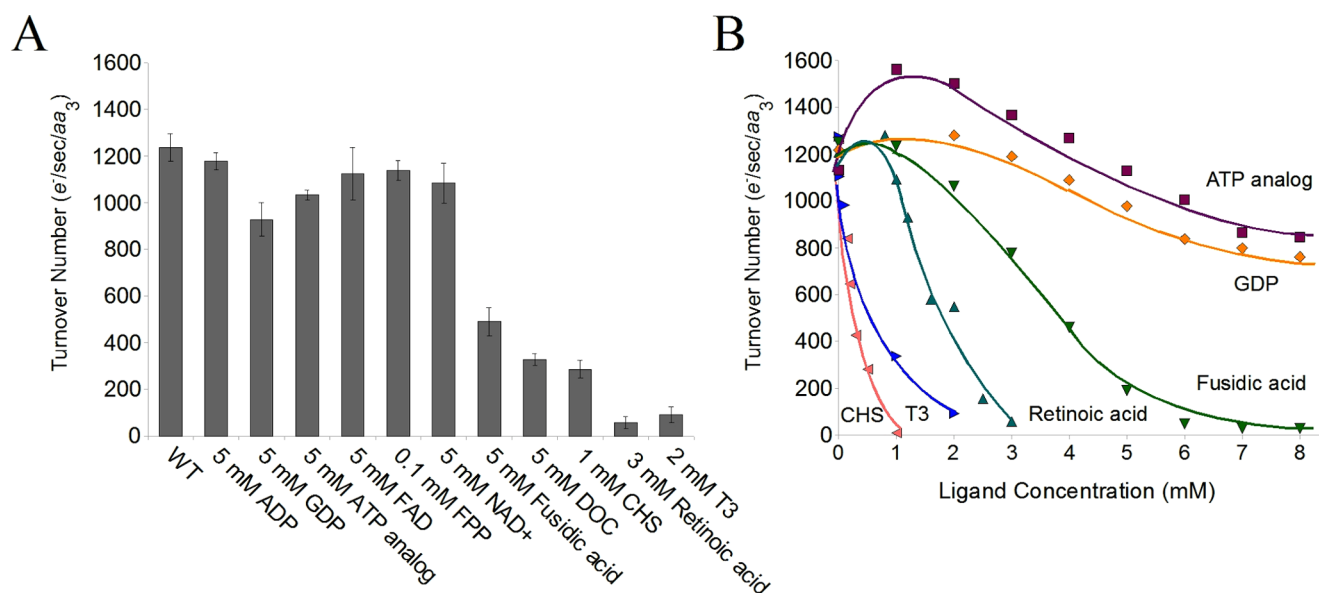


**Figure 5.** An ATP analog and GDP elicit a low level of RsCcO inhibition, while fusidic acid, deoxycholate, cholesterol hemisuccinate, retinoic acid, and T3 thyroid hormone inhibit more strongly. (A) The top scoring, commercially available candidate ligands determined by ROCS and/or SimSite3D were tested at maximal concentration for their ability to affect RsCcO activity with saturating levels of cytochrome *c* substrate. Error bars represent standard deviations from at least three independent trials. (B) Candidate ligands that altered RsCcO activity were further investigated under varying ligand concentrations. Assay conditions: 100 mM HEPES pH 7.4, 24 mM KCl, 2.8 mM ascorbate, 1 mM *N,N,N',N'*-tetramethyl-*p*-phenylenediamine (TMPD), 5.6  $\mu$ M EDTA, 0.01% lauryl maltoside (LM), with 30  $\mu$ M cytochrome *c* as the substrate.

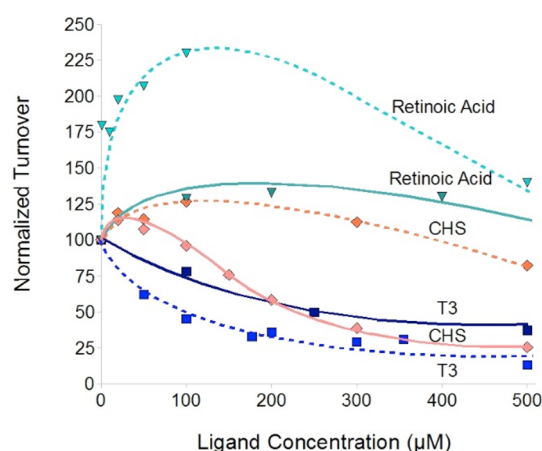


**Figure 6.** Inhibitory ligands differentially affect the RsCcO wild-type and E101A mutant. Ligand effects are determined at saturating levels of cytochrome *c* in both the WT (—) and E101A (---) systems. These effects are normalized to protein activity in the absence of a ligand, approximately 1200 e<sup>-</sup>/s/aa<sub>3</sub> for WT and 600 e<sup>-</sup>/s/aa<sub>3</sub> for the E101A mutant. Retinoic acid (▼) is shown in cyan, CHS (◆) in salmon, and T3 thyroid hormone (■) in blue. Each ligand had a significantly different influence on E101A as compared to WT, consistent with the ligands' influence being due to binding at the bile acid site. Assay conditions as in Figure 5.

oxidized form of the enzyme, affecting K-path proton uptake (see Discussion).

## DISCUSSION

CcO regulates cell metabolism and oxidative phosphorylation efficiency.<sup>14–16</sup> Its function is also controlled through highly regulated expression and assembly<sup>14–16</sup> and tissue specific isoforms.<sup>17,20,21</sup> Eukaryotic CcO is subject to phosphorylation of at least fourteen characterized sites, including three sites on the subunit I–III core.<sup>23</sup> In addition, regulation by adenine

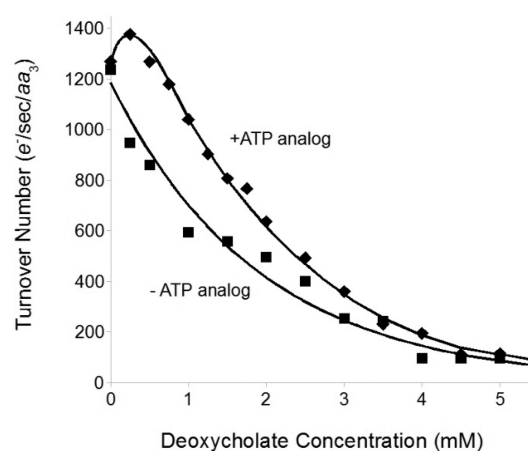


**Figure 7.** Nucleotides bind to the RsCcO bile acid site. The ability of the crystallographically defined DOC ligand to inhibit activity was monitored at saturating levels of cytochrome *c* in the presence and absence of the ATP analog. This analog, at 5 mM concentration, prevented DOC from inhibiting RsCcO activity, presumably because of its ability to compete at the bile acid site. Assay conditions as in Figure 5.

nucleotides<sup>25–27,50,51,53</sup> and other small molecules<sup>25,33,54–57</sup> has been reported. The structural and mechanistic basis of these observed regulatory processes is difficult to investigate in the complex mammalian enzyme. However, the simpler bacterial model system has permitted computational, mutagenic, and functional analyses to characterize small molecule regulation at a conserved bile acid binding site.<sup>33,34</sup>

## Physiological Relevance of Identified CcO Inhibitors.

This work's three-pronged computational approach has identified five candidate ligands that affect CcO activity and have previously been tied to metabolic regulation. Thyroid hormones, including T3, have been shown to stimulate metabolism,<sup>58</sup> to interact specifically with intact mitochondria.

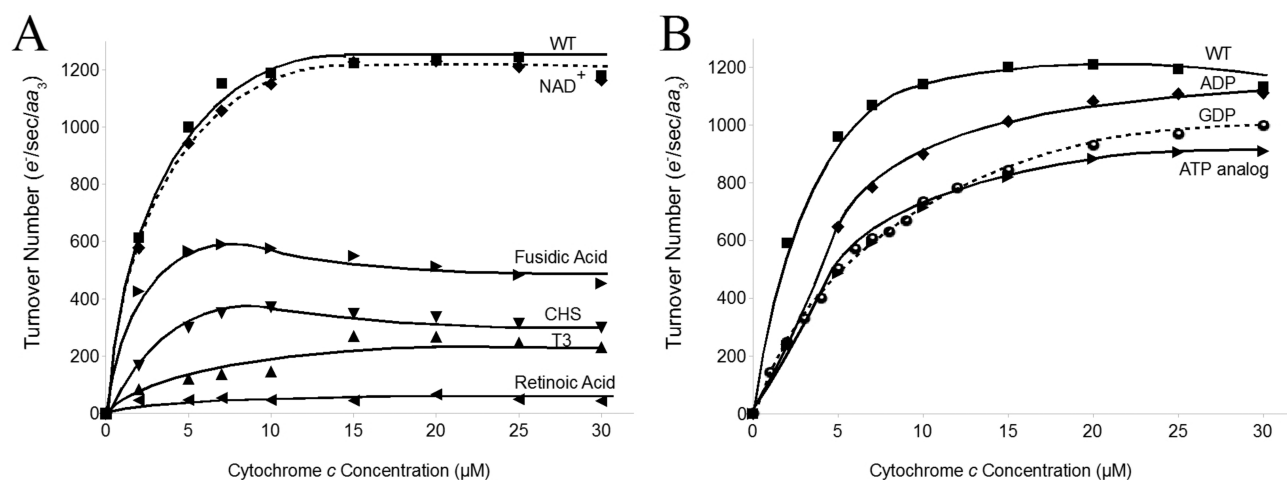


**Figure 8.** Nucleotides inhibit *RsCcO* under low substrate conditions while fusidic acid, retinoic acid, cholesteryl hemisuccinate, and T3 thyroid hormone strongly inhibit activity at all substrate concentrations. Physiological concentrations of all ligands, except for the fusidic acid antibiotic, were tested for their ability to affect *RsCcO* activity under varying concentrations of cytochrome *c* substrate. (A) 5 mM fusidic acid, 250 μM cholesteryl hemisuccinate, 500 μM T3 thyroid hormone, and 1.5 mM retinoic acid ligands strongly inhibit activity in all concentrations of cytochrome *c*. Nicotinamides did not affect enzyme activity. (B) Under low cytochrome *c* conditions, 5 mM ADP, ATP analog, or GDP inhibited the enzyme with sigmoidal behavior, consistent with ATP inhibition of *bovCcO*. Assay conditions as in Figure 5, with 0–30 μM cytochrome *c*.

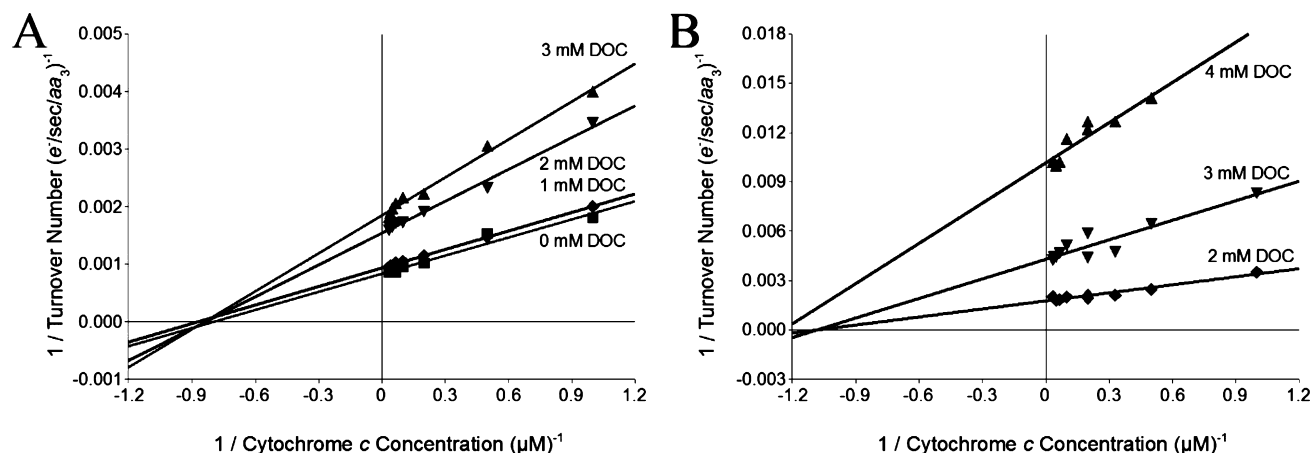


**Figure 9.** Deoxycholate noncompetitively inhibits the *RsCcO* WT and E101A mutant. The double reciprocal plots of activity versus nonsaturating substrate concentration (0–30 μM) are consistent with the noncompetitive inhibition of the *RsCcO* (A) WT and (B) E101A mutant. The *K<sub>m</sub>* of cytochrome *c*, ~1 μM, is unchanged by the DOC inhibition. Assay conditions as in Figure 5, with 0–30 μM cytochrome *c*.

dria,<sup>54,59,60</sup> and to alter *CcO* activity.<sup>61,62</sup> Retinoic acid, the degradative product of the essential vitamin A, has been tied to mitochondrial functions including transcriptional regulation, thermogenesis, and apoptosis.<sup>63,64</sup> High ratios of ATP/ADP, but not other nucleotides,<sup>50</sup> have been shown to inhibit mammalian *CcO*.<sup>25,26,51</sup> Additionally, fusidic acid, a porphyrin-binding mimic,<sup>65</sup> has been identified as a *CcO* inhibitor. It is important to note that porphyrin molecules are not present in the Binding MOAD database and were therefore not evaluated by ROCS or *SimSite3D*. However, protoporphyrin IX and bilirubin have been previously shown to strongly interact with the *CcO* bile acid site and affect activity.<sup>33</sup> One interpretation of these results is that the conserved bile acid site is a polyspecific regulatory site whose ligands may include ATP, GDP, steroids, retinoic acid, T3 thyroid hormone, and porphyrins. This site may then regulate oxidative phosphorylation based on local energetic demand using a varied set of ligands, whose abundance, affinity, and effects will depend on the tissue, the nuclear-encoded subunit isoform, and the metabolic state. It is interesting to note that *bovCcO* subunit VIa impacts directly on

the bile acid binding site<sup>30</sup> and could modify the binding site's specificity through subunit phosphorylation.<sup>23,24</sup> In addition, the location of the bile acid site in *bovCcO* is at the crystallographic dimer interface and in proximity to a cardiolipin site, raising further possibilities of variable ligand specificity and regulatory influence on supercomplex formation.<sup>48</sup>

**Ligand Binding to the *CcO* Bile Acid Site May Arrest the Protein's Active Site in an Oxidized State.** Previous work concluded that the nature of the regulatory effect of bile acid site ligands involved inhibition of the K proton uptake path.<sup>33</sup> In the fully active enzyme starting from the oxidized state, transfer of the first two electrons from cytochrome *c* results in a reduced active site (heme *a*<sub>3</sub><sup>2+</sup>/Cu<sub>B</sub><sup>1+</sup>) which can then bind oxygen and proceed with catalysis of oxygen reduction.<sup>3,66</sup> In contrast, inhibition of the K-path favors retention of electrons by heme *a* and Cu<sub>A</sub> such that the active site is not reduced and has low affinity for oxygen.<sup>33,35–37</sup> This inhibited state is observed spectrally as an increased steady-state ratio of reduced heme *a* to reduced heme *a*<sub>3</sub> upon ligand



binding to the bile acid site or mutation of K-path residues.<sup>33,36,37</sup> The simplest interpretation of these observations is a direct block of K-path-dependent reduction of heme  $a_3$ . If, instead, ligand binding allosterically inhibited the D proton uptake path, irreversible suicide inactivation would be expected.<sup>67,68</sup> However, this phenomenon is not observed. Therefore, by regulating CcO through the K-path, enzyme activity can be controlled transiently in response to changing physiological conditions without altering the enzyme's integrity.

Two hypotheses have been proposed for the mechanism of K-path inhibition.<sup>33</sup> First, mutations and ligand binding to the bile acid site may disrupt or constrain dynamic water molecules likely required for proton conductance in the K-path.<sup>33,34,69</sup> Indeed, the RsCcO crystal structure in the DOC-bound state shows an increased number of well-resolved, stable water molecules in the K-path entry.<sup>31</sup> Second, mutations and ligand binding may restrict conformational change of subunit I helix VIII,<sup>33</sup> which has been shown to be flexible by crystallography,<sup>70</sup> solvent accessibility,<sup>71</sup> and intrinsic flexibility calculations.<sup>72</sup> The latter hypothesis is further supported by crystallographic studies indicating preferential binding of DOC to the oxidized form<sup>33</sup> and the sigmoidal kinetics of nucleotide inhibition (Figure 8B), suggesting that at low cytochrome  $c$  concentrations (hence more oxidized state) the ligands bind with greater affinity.

A plausible rationale for controlling CcO via affecting the K-path may be understood by considering the conservation of this path and its role in the catalytic cycle. The K-path is the only proton uptake path conserved in heme/copper oxidases from bacteria to mammals.<sup>73,74</sup> Therefore, the K-path represents both an ancestral and a conserved target for regulation. Further, by blocking the K-path, the enzyme is arrested in a semioxidized state ( $\text{Cu}_A$ , heme  $a$  reduced;  $\text{Cu}_B$ , heme  $a_3$  oxidized), which has a low affinity for  $\text{O}_2$  binding,<sup>66,75,76</sup> lessening the probability of forming damaging reactive oxygen species. Indeed, a form of boVCcO with slowed turnover, a similar decreased heme  $a$  to  $a_3$  electron transfer rate, and an oxidized active site has been previously characterized as the "resting" or "slow" form of CcO.<sup>77–82</sup> We suggest that this commonly observed state could represent a form in which a detergent, such as cholate, or other ligand is already occupying the bile acid site. A similar hypothesis was previously proposed<sup>82</sup> with respect to another bile acid binding site that is also at the dimer interface of the bovine enzyme, but is not conserved in the bacterial form. However, unlike the boVCcO resting form,<sup>78–82</sup> a spectral shift in the Soret band is not observed in the ligand-inhibited RsCcO,<sup>33</sup> and the EPR and cyanide binding characteristics of the inhibited bacterial form have yet to be explored.

## CONCLUSIONS

Three complementary computational methods have been applied in this study to predict possible physiological ligands for the conserved CcO bile acid site. *In vitro* oxygen consumption assays validated an ATP analog, GDP, cholesteryl hemisuccinate, retinoic acid, and T3 thyroid hormone as inhibitors of RsCcO. Porphyrin ligands are also implicated based on the prediction of the porphyrin mimic fusidic acid and previous evidence of porphyrin regulation.<sup>33</sup> These ligands were confirmed to interact at or near the bile acid site based on their differential effects on the bile acid binding site mutant, E101A, and competition with the crystallographically identified ligand, DOC. This work provides an initial characterization of

bacterial CcO regulation by nucleotides, exhibiting sigmoidal kinetics reminiscent of the ATP inhibition of mammalian CcO and ties this regulation to the bile acid site on the enzyme's core subunits, common to both bacterial and mammalian oxidases.

We propose ligand binding at the bile acid site, which is noncompetitive with respect to cytochrome  $c$ , affects CcO activity by altering the K-path dependent proton uptake. This can result in the arrest of CcO in a form resembling a "resting" state, where the active site is oxidized and has little potential for generating oxygen radical byproducts. The location and conservation of the binding site and the regulatory response suggest that small molecule interactions at the bile acid site may be an important mechanism of modulating oxidative phosphorylation.

## ASSOCIATED CONTENT

### Supporting Information

Supporting Information includes compete ranked ROCS and SimSite3D results, kinetic fit parameters, and 2D ligand representations. This material is available free of charge via the Internet at <http://pubs.acs.org>.

## AUTHOR INFORMATION

### Corresponding Authors

\*Tel.: 001 517 355 0199. E-mail: [fergus20@msu.edu](mailto:fergus20@msu.edu).

\*Tel.: 001 517 353 8745. Fax: 001 517 353 9334. E-mail: [KuhnL@msu.edu](mailto:KuhnL@msu.edu). Web: <http://www.kuhnlab.bmb.msu.edu>.

### Funding

<sup>†</sup>This work was supported by NIH GM26916 to S.F.-M and includes data with permission from Buhrow, L., Ph.D. dissertation. Computational prediction and experimental validation of cytochrome  $c$  oxidase main-chain flexibility and allosteric regulation of the K-pathway. Michigan State University, United States – Michigan. (Publication No. AAT 3549123).

### Notes

The authors declare no competing financial interest.

## ACKNOWLEDGMENTS

The authors thank OpenEye Scientific Software (Santa Fe, NM) for providing an academic license for the use of ROCS and Omega software.

## ABBREVIATIONS

boVCcO, Bovine CcO; CHS, cholesteryl hemisuccinate; CcO, cytochrome  $c$  oxidase; DOC, deoxycholate; LM, lauryl maltoside ( $n$ -dodecyl- $\beta$ -D-maltoside); RsCcO, *Rhodobacter sphaeroides* CcO; TMPD,  $N,N,N',N'$ -tetramethyl- $p$ -phenylenediamine; WT, wild-type; FPP, farnesyl diphosphate

## REFERENCES

- (1) Hosler, J. P., Ferguson-Miller, S., and Mills, D. A. (2006) Energy transduction: Proton transfer through the respiratory complexes. *Annu. Rev. Biochem.* 75, 165–187.
- (2) Ferguson-Miller, S., and Babcock, G. T. (1996) Heme/copper terminal oxidases. *Chem. Rev.* 96, 2889–2908.
- (3) Brändén, M., Tomson, F., Gennis, R. B., and Brzezinski, P. (2002) The entry point of the K-proton-transfer pathway in cytochrome  $c$  oxidase. *Biochemistry* 41, 10794–10798.
- (4) Ruitenbergh, M. R., Aimo, K., Bamberg, E., Fendler, K., and Michel, H. (2002) Reduction of cytochrome  $c$  oxidase by a second electron leads to proton translocation. *Nature* 417, 99–102.

- (5) Bloch, D., Belevich, I., Jasaitis, A., Ribacka, C., Puustinen, A., and Verkhovskiy, M. I. (2004) The catalytic cycle of cytochrome *c* oxidase is not the sum of its two halves. *Proc. Natl. Acad. Sci. U.S.A.* 101, 529–533.
- (6) Luna, V. M., Chen, Y., Fee, J. A., and Stout, C. D. (2008) Crystallographic studies of Xe and Kr binding within the large internal cavity of cytochrome *ba*3 from *Thermus thermophilus*: Structural analysis and role of oxygen transport channels in the heme–cu oxidases. *Biochemistry* 47, 4657–4665.
- (7) Luna, V. M., Fee, J. A., Deniz, A. A., and Stout, C. D. (2012) Mobility of Xe atoms within the oxygen diffusion channel of cytochrome *ba*(3) oxidase. *Biochemistry* 51, 4669–4676.
- (8) Qian, J., Mills, D. A., Geren, L., Wang, K., Hoganson, C. W., Schmidt, B., Hiser, C., Babcock, G. T., Durham, B., Millett, F., and Ferguson-Miller, S. (2004) Role of the conserved arginine pair in proton and electron transfer in cytochrome *c* oxidase. *Biochemistry* 43, 5748–5756.
- (9) Mills, D. A., Geren, L., Hiser, C., Schmidt, B., Durham, B., Millett, F., and Ferguson-Miller, S. (2005) An arginine to lysine mutation in the vicinity of the heme propionates affects the redox potentials of the hemes and associated electron and proton transfer in cytochrome *c* oxidase. *Biochemistry* 44, 10457–10465.
- (10) Seibold, S. A., Mills, D. A., Ferguson-Miller, S., and Cukier, R. I. (2005) Water chain formation and possible proton pumping routes in *Rhodobacter sphaeroides* cytochrome *c* oxidase: A molecular dynamics comparison of the wild type and R481K mutant. *Biochemistry* 44, 10475–10485.
- (11) Egawa, T., Lee, H. J., Gennis, R. B., Yeh, S.-R., and Rousseau, D. L. (2009) Critical structural role of R481 in cytochrome *c* oxidase from *Rhodobacter sphaeroides*. *Biochim. Biophys. Acta* 1787, 1271–1275.
- (12) Lee, H. J., Ojemyr, L., Vakkasoglu, A., Brzezinski, P., and Gennis, R. B. (2009) Properties of Arg481 mutants of the *aa*3-type cytochrome *c* oxidase from *Rhodobacter sphaeroides* suggest that neither R481 nor the nearby D-propionate of heme *a*3 is likely to be the proton loading site of the proton pump. *Biochemistry* 48, 7123–7131.
- (13) Popović, D. M., and Stuchebrukhov, A. A. (2006) Proton exit channels in bovine cytochrome *c* oxidase. *J. Phys. Chem. B* 109, 1999–2006.
- (14) Pacelli, C., Latorre, D., Cocco, T., Capuano, F., Kukut, C., Seibel, P., and Villani, G. (2011) Tight control of mitochondrial membrane potential by cytochrome *c* oxidase. *Mitochondrion* 11, 334–341.
- (15) Villani, G., and Attardi, G. (1997) *In vivo* control of respiration by cytochrome *c* oxidase in wild-type and mitochondrial DNA mutation-carrying human cells. *Proc. Natl. Acad. Sci. U.S.A.* 94, 166–171.
- (16) Hüttemann, M., Helling, S., Sanderson, T. H., Sinkler, C., Samaviti, L., Mahapatra, G., Varughese, A., Lu, G., Liu, J., Grossman, L. I., Doan, J. W., Marcus, K., and Lee, I. (2012) Regulation of mitochondrial respiration and apoptosis through cell signaling: Cytochrome *c* oxidase and cytochrome *c* in ischemia/reperfusion injury and inflammation. *Biochim. Biophys. Acta* 1817, 598–609.
- (17) Pierron, D., Wildman, D. E., Hüttemann, M., Markondapatnaikuni, G. C., Aras, S., and Grossman, L. I. (2012) Cytochrome *c* oxidase: Evolution of control via nuclear subunit addition. *Biochim. Biophys. Acta* 1817, 590–597.
- (18) Das, J., Miller, S. T., and Stern, D. L. (2004) Comparison of diverse protein sequences of the nuclear-encoded subunits of cytochrome *c* oxidase suggest conservation of structure underlies evolving functional sites. *Mol. Biol. Evol.* 21, 1572–1582.
- (19) LaMarche, A. E. P., Abate, M. I., Chan, S. H. P., and Trumpower, B. L. (1992) Isolation and characterization of COX12, the nuclear gene for a previously unrecognized subunit of *Saccharomyces cerevisiae* cytochrome *c* oxidase. *J. Biol. Chem.* 276, 22473–22480.
- (20) Hüttemann, M., Kadenbach, B., and Grossman, L. I. (2001) Mammalian subunit IV isoforms of cytochrome *c* oxidase. *Gene* 267, 111–123.
- (21) Hüttemann, M., Schmidt, T. R., and Grossman, L. I. (2003) A third form of cytochrome *c* oxidase subunit VII is present in mammals. *Gene* 312, 95–102.
- (22) Grossman, L. I., and Lomax, M. I. (1997) Nuclear encoded genes for cytochrome *c* oxidase. *Biochim. Biophys. Acta* 1352, 174–192.
- (23) Hüttemann, M., Lee, I., Grossman, L. I., Doan, J. W., and Sanderson, T. H. (2012) Phosphorylation of mammalian cytochrome *c* and cytochrome *c* oxidase in the regulation of cell destiny: Respiration, apoptosis, and human disease. *Adv. Exp. Med. Biol.* 748, 237–264.
- (24) Fang, J. K., Prabu, S. K., Sepuri, N. B., Raza, H., Anandatheerthavarada, H. K., Galati, D., Spear, J., and Avadhani, N. G. (2007) Site specific phosphorylation of cytochrome *c* oxidase subunits I, IVi1, and Vb in rabbit hearts subjected to ischemia/reperfusion. *FEBS Lett.* 581, 1302–1310.
- (25) Arnold, S., Goglia, F., and Kadenbach, B. (1998) 3,5-Diiodothyronine binds to subunit Va of cytochrome-*c* oxidase and abolishes the allosteric inhibition of respiration by ATP. *Eur. J. Biochem.* 252, 325–330.
- (26) Arnold, S., and Kadenbach, B. (1997) Cell respiration is controlled by ATP, an allosteric inhibitor of cytochrome-*c* oxidase. *Eur. J. Biochem.* 249, 350–354.
- (27) Bender, E., and Kadenbach, B. (2000) The allosteric ATP-inhibition of cytochrome *c* oxidase activity is reversibly switched on by cAMP-dependent phosphorylation. *FEBS Lett.* 466, 130–134.
- (28) Lee, I., Bender, E., and Kadenbach, B. (2002) Control of mitochondrial membrane potential and ROS formation by reversible phosphorylation of cytochrome *c* oxidase. *Mol. Cell. Biochem.* 234–235, 63–70.
- (29) Lee, I., Salomon, A. R., Ficarro, S., Mathes, I., Lottspeich, F., Grossman, L. I., and Hüttemann, M. (2005) cAMP-dependent tyrosine phosphorylation of subunit I inhibits cytochrome *c* oxidase activity. *J. Biol. Chem.* 280, 6094–6100.
- (30) Tsukihara, T., Aoyama, H., Yamashita, E., Tomizaki, T., Yamaguchi, H., Shinzawa-Itoh, K., Nakashima, R., Yaono, R., and Yoshikawa, S. (1996) The whole structure of the 13-subunit oxidized cytochrome *c* oxidase at 2.8 angstrom. *Science* 272, 1136–1144.
- (31) Qin, L., Mills, D. A., Buhrow, L., Hiser, C., and Ferguson-Miller, S. (2008) A conserved steroid binding site in cytochrome *c* oxidase. *Biochemistry* 47, 9931–9933.
- (32) Hosler, J. P., Fetter, J., Tecklenburg, M. M. J., Espe, M., Lerma, C., and Ferguson-Miller, S. (1992) Cytochrome-*aa*3 of *Rhodobacter sphaeroides* as a model for mitochondrial cytochrome *c* oxidase - Purification, kinetics, proton pumping, and spectral analysis. *J. Biol. Chem.* 267, 24264–24272.
- (33) Hiser, C., Buhrow, L., Liu, J., Kuhn, L., and Ferguson-Miller, S. (2013) A conserved amphipathic ligand binding region influences K-path-dependent activity of cytochrome *c* oxidase. *Biochemistry* 52, 1385–1396.
- (34) Ferguson-Miller, S., Hiser, C., and Liu, J. (2012) Gating and regulation of the cytochrome *c* oxidase proton pump. *Biochim. Biophys. Acta* 1817, 489–494.
- (35) Vik, S. B., and Capaldi, R. A. (1977) Lipid requirements for cytochrome-*c* oxidase activity. *Biochemistry* 16, 5755–5759.
- (36) Konstantinov, A. A., Siletsky, S., Mitchell, D., Kaulen, A., and Gennis, R. B. (1997) The roles of the two proton input channels in cytochrome *c* oxidase from *Rhodobacter sphaeroides* probed by the effects of site-directed mutations on time-resolved electrogenic intraprotein proton transfer. *Proc. Natl. Acad. Sci. U.S.A.* 94, 9085–9090.
- (37) Antalík, M., Jancura, D., Palmer, G., and Fabian, M. (2005) A role for the protein in internal electron transfer to the catalytic center of cytochrome *c* oxidase. *Biochemistry* 44, 14881–14889.
- (38) Hawkins, P. C. D., Skillman, A. G., and Nicholls, A. (2007) Comparison of shape-matching and docking as virtual screening tools. *J. Med. Chem.* 50, 74–82.
- (39) Grant, J. A., Gallardo, M. A., and Pickup, B. T. (1996) A fast method of molecular shape comparison: A simple application of a Gaussian description of molecular shape. *J. Comput. Chem.* 17, 1653–1666.

- (40) Van Voorst, J. R. (2011) *Surface matching and chemical scoring to detect unrelated proteins binding similar small molecules*, Ph.D. thesis, Michigan State University, 3465552.
- (41) Schnecke, V., Swanson, C. A., Getzoff, E. D., Tainer, J. A., and Kuhn, L. A. (1998) Screening a peptidyl database for potential ligands to proteins with side-chain flexibility. *Proteins* 33, 74–87.
- (42) Zavodszky, M. I., Sanschagrin, P. C., Korde, R. S., and Kuhn, L. A. (2002) Distilling the essential features of a protein surface for improving protein-ligand docking, scoring, and virtual screening. *J. Comput.-Aid Mol. Des.* 16, 883–902.
- (43) Benson, M. L., Smith, R. D., Khazanov, N. A., Dimcheff, B., Beaver, J., Dresslar, P., Nerothin, J., and Carlson, H. A. (2007) Binding MOAD, a high-quality protein-ligand database. *Nucleic Acids Res.* 36, D674–D678.
- (44) Hawkins, P. C. W., Skillman, A. G., Warren, G. L., Ellingson, B. A., and Stahl, M. T. (2010) Conformer generation with OMEGA: Algorithm and validation using high quality structures from the Protein Databank and Cambridge Structural Database. *J. Chem. Inf. Modeling* 50, 572.
- (45) Sanner, M., Olsen, A. J., and Spohner, J. C. (1996) Reduced surface: An efficient way to compute molecular surfaces. *Biopolymers* 38, 305–320.
- (46) Hiser, C., Mills, D. A., Schall, M., and Ferguson-Miller, S. (2001) C-terminal truncation and histidine-tagging of cytochrome *c* oxidase subunit II reveals the native processing site, shows involvement of the C-terminus in cytochrome *c* binding, and improves the assay for proton pumping. *Biochemistry* 40, 1606–1615.
- (47) Qin, L., Sharpe, M. A., Garavito, R. M., and Ferguson-Miller, S. (2007) Conserved lipid-binding sites in membrane proteins: A focus on cytochrome *c* oxidase. *Curr. Opin. Struct. Biol.* 17, 444–450.
- (48) Althoff, T., Deryck, J. M., Popot, J.-L., and Kühlbrandt, W. (2011) Arrangement of electron transport chain components in bovine mitochondrial supercomplex I<sub>1</sub>III<sub>2</sub>IV<sub>1</sub>. *EMBO J.* 30, 4652–4664.
- (49) Beis, I., and Newsholme, E. A. (1975) The contents of adenine nucleotides, phosphagens and some glycolytic intermediates in resting muscles from vertebrates and invertebrates. *Biochemistry* 152, 23–32.
- (50) Napiwotzki, J., Shinzawa-Itoh, K., Yoshikawa, S., and Kadenbach, B. (1997) ATP and ADP bind to cytochrome *c* oxidase and regulate its activity. *Biol. Chem.* 378, 1013–1021.
- (51) Frank, V., and Kadenbach, B. (1996) Regulation of the H<sup>+</sup>/e<sup>(-)</sup> stoichiometry of cytochrome *c* oxidase from bovine heart by intramitochondrial ATP/ADP ratios. *FEBS Lett.* 382, 121–124.
- (52) Buhrow, L. (2012) *Computational prediction and experimental validation of cytochrome *c* oxidase main-chain flexibility and allosteric regulation of the K-pathway*, Ph.D. thesis, Michigan State University, 3549123.
- (53) Follmann, K., Arnold, S., Ferguson-Miller, S., and Kadenbach, B. (1998) Cytochrome *c* oxidase from eucaryotes but not from procaryotes is allosterically inhibited by ATP. *Biochem. Mol. Biol. Int.* 45, 1047–1055.
- (54) Goglia, F., Lanni, A., Horst, C., Moreno, M., and Thoma, R. (1994) In vitro binding of 3,5-di-iodo-L-thyronine to rat liver mitochondria. *J. Mol. Endocrinol.* 13, 275–282.
- (55) Simon, N., Joliet, P., Morin, C., Zini, R., Urien, S., and Tillement, J. P. (1998) Glucocorticoids decrease cytochrome *c* oxidase activity of isolated rat kidney mitochondria. *FEBS Lett.* 435, 25–28.
- (56) Vaz, A. R., Delgado-Esteban, M., Brito, M. A., Bolanos, J. P., Brites, D., and Almeida, A. (2010) Bilirubin selectively inhibits cytochrome *c* oxidase activity and induces apoptosis in immature cortical neurons: assessment of the protective effects of glycourso-deoxycholic acid. *J. Neurochem.* 112, 56–65.
- (57) Malik, S. G., Irwanto, K. A., Ostrow, J. D., and Tiribelli, C. (2010) Effect of bilirubin on cytochrome *c* oxidase activity of mitochondria from mouse brain and liver. *BMC Res. Notes* 3, 162–167.
- (58) Moreno, M., Lanni, A., Lombardi, A., and Goglia, F. (1997) How the thyroid controls metabolism in the rat: Different roles for triiodothyronine and diiodothyronines. *J. Physiol.* 505, 529–538.
- (59) Lanni, A., Moreno, M., Cioffi, M., and Goglia, F. (1993) Effect of 3,3'-diiodothyronine and 3,5'-diiodothyronine on rat liver mitochondria. *J. Endocrinol.* 136, 59–64.
- (60) Lanni, A., Moreno, M., Horst, C., Lombardi, A., and Goglia, F. (1994) Specific binding sites for 3,3'-diiodo-L-thyronine (3,3'-T<sub>2</sub>) in rat liver mitochondria. *FEBS Lett.* 351, 237–240.
- (61) Goglia, F., Lanni, A., Barth, J., and Kadenbach, B. (1994) Interaction of diiodothyronine with isolated cytochrome *c* oxidase. *FEBS Lett.* 346, 295–298.
- (62) Lanni, A., Moreno, A., Lombardi, A., and Goglia, F. (1994) Rapid stimulation in vitro of rat liver cytochrome oxidase activity by 3,5-diiodo-L-thyronine and by 3,3'-diiodo-L-thyronine. *Mol. Cell. Endocrinol.* 99, 89–94.
- (63) Lowell, B. B., and Spiegelman, B. M. (2000) Towards a molecular understanding of adaptive thermogenesis. *Nature* 404, 652–660.
- (64) Noy, N. (2010) Between death and survival: Retinoic acid in regulation of apoptosis. *Annu. Rev. Nutr.* 30, 201–217.
- (65) Zunszain, P. A., Ghuman, J., McDonagh, A. F., and Curry, S. (2008) Crystallographic analysis of human serum albumin complexed with 4Z,15E-bilirubin-IX alpha. *J. Mol. Biol.* 381, 394–406.
- (66) Sharpe, M. A., and Ferguson-Miller, S. (2008) A chemically explicit model for the mechanism of proton pumping in heme-copper oxidases. *J. Bioenerg. Biomembr.* 40, 541–549.
- (67) Bratton, M. R., Pressler, M. A., and Hosler, J. P. (1999) Suicide inactivation of cytochrome *c* oxidase: Catalytic turnover in the absence of subunit III alters the active site. *Biochemistry* 38, 16236–16245.
- (68) Mills, D. A., and Hosler, J. P. (2005) Slow proton transfer through the pathways for pumped protons in cytochrome *c* oxidase induces suicide inactivation of the enzyme. *Biochemistry* 44, 4656–4666.
- (69) Koepke, J., Olkhova, E., Angerer, H., Muller, H., Peng, G., and Michel, H. (2009) High resolution crystal structure of *Paracoccus denitrificans* cytochrome *c* oxidase: New insights into the active site and the proton transfer pathways. *Biochim. Biophys. Acta* 1787, 635–645.
- (70) Qin, L., Liu, J., Mills, D. A., Proshlyakov, D. A., Hiser, C., and Ferguson-Miller, S. (2009) Redox-dependent conformational changes in cytochrome suggest a gating mechanism for proton uptake. *Biochemistry* 48, 5121–5130.
- (71) Busenlehner, L. S., Salomonsson, L., Brzezinski, P., and Armstrong, R. N. (2006) Mapping protein dynamics in catalytic intermediates of the redox-driven proton pump cytochrome *c* oxidase. *Proc. Natl. Acad. Sci. U.S.A.* 103, 15398–15403.
- (72) Buhrow, L., Ferguson-Miller, S., and Kuhn, L. A. (2012) From static structure to living protein, Computational analysis of cytochrome *c* oxidase main-chain flexibility. *Biophys. J.* 102, 2158–2166.
- (73) Tiefenbrunn, T., Liu, W., Chen, Y., Katritch, V., Stout, C. D., Fee, J. A., and Cherezov, Y. (2011) High resolution structure of the *ba3* cytochrome *c* oxidase from *Thermus thermophilus* in lipid environment. *Plos ONE* 6, e22348–e22348.
- (74) Hemp, J., and Gennis, R. B. (2008) Diversity of the heme-copper superfamily in archaea: Insights from genomics and structural modeling. *Results Probl. Cell. Differ.* 45, 1–31.
- (75) Verkhovsky, M. I., Morgan, J. E., and Wikstrom, M. (1994) Oxygen binding and activation: Early steps in the reaction of oxygen with cytochrome *c* oxidase. *Biochemistry* 33, 3079–3086.
- (76) Brzezinski, P., and Gennis, R. B. (2008) Cytochrome *c* oxidase: Exciting progress and remaining mysteries. *Bioenerg. Biomembr.* 40, 521–531.
- (77) Antonini, E., Brunori, M., Colosimo, A., Greenwood, C., and Wilson, M. T. (1977) Oxygen “pulsed” cytochrome *c* oxidase: Functional properties and catalytic relevance. *Proc. Natl. Acad. Sci. U.S.A.* 74, 3128–3132.
- (78) Brunori, M., Colosimo, A., Rainoni, G., Wilson, M. T., and Antonini, E. (1979) Functional intermediates of cytochrome oxidase. Role of “pulsed” oxidase in the pre-steady state and steady state reactions of the beef enzyme. *J. Biol. Chem.* 254, 10769–10775.



- (79) Brudvig, G. W., Stevens, T. H., Morse, R. H., and Chan, S. I. (1981) Conformations of oxidized cytochrome *c* oxidase. *Biochemistry* 20, 3912–3921.
- (80) Moody, A. J., Cooper, C. E., and Rich, P. R. (1991) Characterization of 'fast' and 'slow' forms of bovine heart cytochrome-*c* oxidase. *Biochim. Biophys. Acta* 1059, 189–207.
- (81) Schoonover, J. R., and Palmer, G. (1991) Reaction of formate with the fast form of cytochrome oxidase: A model for the fast to slow conversion. *Biochemistry* 30, 7541–7550.
- (82) Shoji, K., Giuffre, A., D'Itri, E., Hagiwara, K., Yamanaka, T., Brunori, M., and Sarti, P. (2000) The ratio between the fast and slow forms of bovine cytochrome *c* oxidase is changed by cholate or nucleotides bound to the cholate-binding site close to the cytochrome *a*<sub>3</sub>:CuB binuclear centre. *Cell. Mol. Life Sci.* 57, 1482–1487.
- (83) Roberts, V. A., and Pique, M. E. (1999) Definition of the interaction domain for cytochrome *c* on cytochrome *c* oxidase: III. Prediction of the docked complex by complete, systematic search. *J. Biol. Chem.* 274, 38051–38060.